ENDOR Spectroscopy of Ion Pairs derived from Tropones and Alkali Metals: Evidence for Stereoisomerism

M. Luisa T. M. B. Franco, M. Celina R. L. R. Lazana, and Bernardo J. Herold *
Instituto Superior Técnico, Laboratório de Química Orgânica, Av. Rovisco Pais, P-1096 Lisboa Codex, Portugal

ESR and ENDOR/TRIPLE resonance studies are reported for the ion pairs derived from the non-planar ketyls of tribenzotropone (**1**), dibenzotropone (**2**) and dibenzosuberone (**3**) with different alkali metal cations. The observation of three different alkali hyperfine splitting constants (hfs) in some ENDOR spectra may indicate the presence of three different stereoisomers of these ion pairs. All hfs data and their temperature dependence can be interpreted in terms of three different ion pair structures. The proton hfs are well interpreted in terms of McLachlan's spin-density calculations. Support for the geometries proposed for the three stereoisomers is provided by INDO calculations of the spin densities at the lithium cation.

The importance in chemistry and biology of single electron transfer reactions involving organic molecules has been increasingly recognised and has revived interest in the relation between structure and reactivity in ion pairs of radical ions in solution. In this context, the position of the metal cation, relative to its associated radical anion, is particularly important.

The direct determination of the cation position by single-crystal X-ray diffraction has been carried out in only a few cases and mainly for aromatic hydrocarbon ion pairs or similar ones where the metal cation is loosely bound to the radical anion.[1–3] Bock *et al.*[4] have recently reported the first determination for a crystal obtained from a solution of a radical-contact ion pair, *i.e.* the sodium fluorenone (Fl) ketyl in dimethoxyethane (DME). The structure is that of a dimer $[Fl^{-\bullet}Na^{+}(DME)_2]_2$ where two negatively charged oxygen atoms and two sodium cations lie in a parallelogram with O–Na distances of 2.28 and 2.40 Å. However, the single-crystal X-ray structure of the dimer reflects only to a certain degree the structure of the monomer in solution. Nevertheless, the information provided is very useful when attempting to establish the structure of the ion pair by other methods.

For several reasons, not least that the solutions of these ion pairs are extremely air- and moisture-sensitive, it is very difficult to obtain good crystals for the X-ray determination. The structures of such ion pairs, therefore, have to be studied by other relevant spectroscopic techniques. From an experimental point of view, the ESR hyperfine splitting (hfs) constants in radical ion pairs (where the relative signs are available from ENDOR and TRIPLE resonance measurements) provide the most relevant information about the stereochemistry of these ion pairs. The signs of the cation hfs constants and their variation with the temperature and the nature of the solvent are particularly important for the prediction of the cation position in the ion pairs.

Among the different theoretical models used to elucidate the structure of the ion pair, the INDO calculations seem to give the most realistic assignment of the hfs constants. Besides the location of the cation, there is always uncertainty in the geometry of the radical anion and one normally assumes the standard ground-state geometry of the neutral molecule before reduction (when available from the crystal structure) since an optimisation of radical geometry with respect to total energy is not practicable for large molecules.

Earlier INDO calculations on ion pairs dealt with naphthalene–lithium,[5] 4-nitropyridine–lithium,[6] and fluorenone–lithium.[7] In the structure proposed by Lubitz *et al.*[7] for the fluorenone ketyl, assuming for the ketyl the crystal structure obtained for unreduced fluorenone, the lithium cation is located above the carbonyl group, closer to the carbon atom of the fluorene ring than to the oxygen atom. In all the ion pairs above, the planar radical anion renders the association of the counter-ion equally probable from both sides of the plane of the molecule, leading to structurally indistinguishable ion pairs. In order to make the two sides of the radical anion topologically distinguishable, a system with a non-planar ring may be suitable. A seven-membered ring ketone seemed a good example to investigate the occurrence of different stereoisomers when ion-pair association occurs.

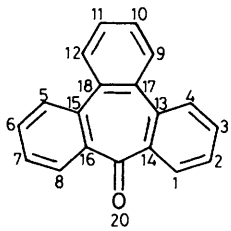

(1)

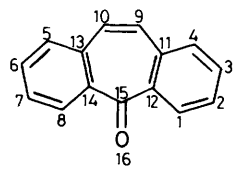

(2)

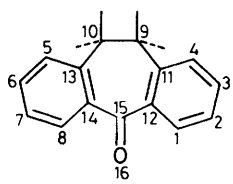

(3)

The electrolytical reduction of dibenzosuberone as well as the reduction of dibenzotropone either electrolytically or with alkali metals has been studied using ESR by Tabner *et al.*[8] They were interested in the study of the radical anions and proton hfs constants only. A small potassium hfs for $(dibenzotropone)^{-\bullet}K^{+}$ was measured at 203 K. No reference is made in this work to the occurrence of different stereoisomers.

Here we report a study of the reduction of tribenzotropone (**1**) with different alkali metals. Increased stability of the ion pairs derived from (**1**) due to the larger aromatic system may be expected. Thus not only can the study be extended to a larger range of temperatures but also better-resolved ESR spectra can be expected. The reductions of dibenzotropone (**2**) and

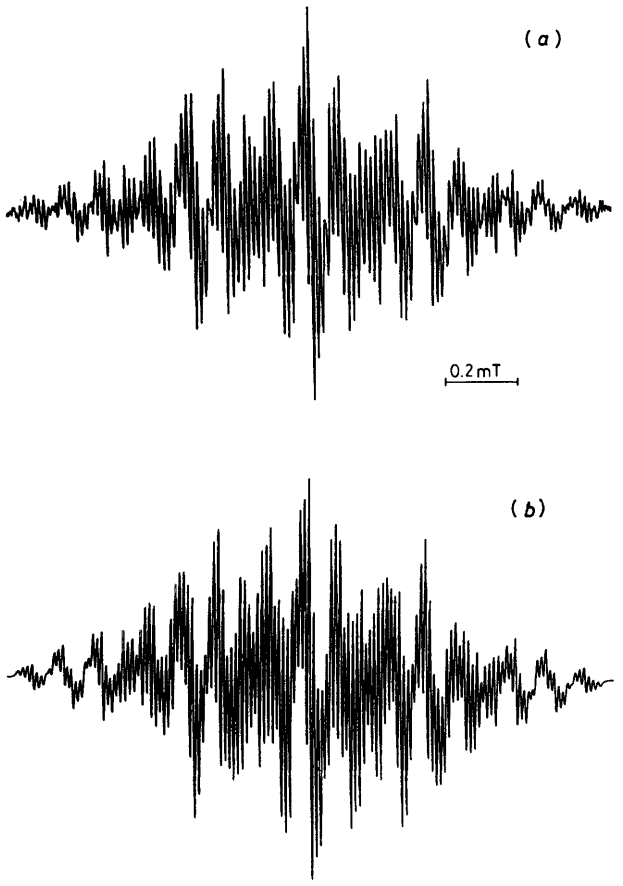

Figure 1. ESR spectrum of $(1)^{-\bullet}$ in DMF at room temperature: (*a*) experimental; (*b*) simulated with line width 0.007 mT.

dibenzosuberone (**3**) with alkali metals have also been reinvestigated.

Results

The cyclic voltammogram of tribenzotropone (**1**) in dimethylformamide (DMF) displays a first reversible reduction wave with half-wave potential $E_{\frac{1}{2}} = -1.7$ *V* (*vs.* SCE) showing the appearance of a radical anion with high kinetic stability. A very intense and well resolved ESR spectrum of $(1)^{-\bullet}$ is readily obtained by electrolytical reduction of (**1**) in DMF. This spectrum presents a complex hyperfine pattern due to the interaction of the single electron with six pairs of protons (Figure 1).

The reduction of (**1**) with all the alkali metals in ethereal solvents leads to the formation of very persistent paramagnetic ion pairs $[(1)^{-\bullet}M^+]$ (M = Li, Na, K, Rb, Cs) with well resolved and very complex ESR spectra. The ESR studies were conducted between 178 K and room temperature. The ESR spectra of potassium and caesium ion pairs are easily simulated with the proton hfs constants obtained from the simulation of $(1)^{-\bullet}$ (Figure 1) and only one small hfs from the alkali metal. The ESR spectra of the ion pairs derived from Li, Na, and Rb differ strikingly in the fact that they are even more complex and could not be simulated under the above conditions. In fact, the high resolution of their ESR spectra allows a confident analysis of the outermost groups of lines and the determination of the total length of the hyperfine pattern. However, it is significant that the simulations based on the alkali hfs constants obtained in this way together with the protonic hfs of $(1)^{-\bullet}$ do not reproduce the experimental spectra. For $[(1)^{-\bullet}Rb^+]$ the simulation of the ESR spectra is even more difficult due to the existence of two

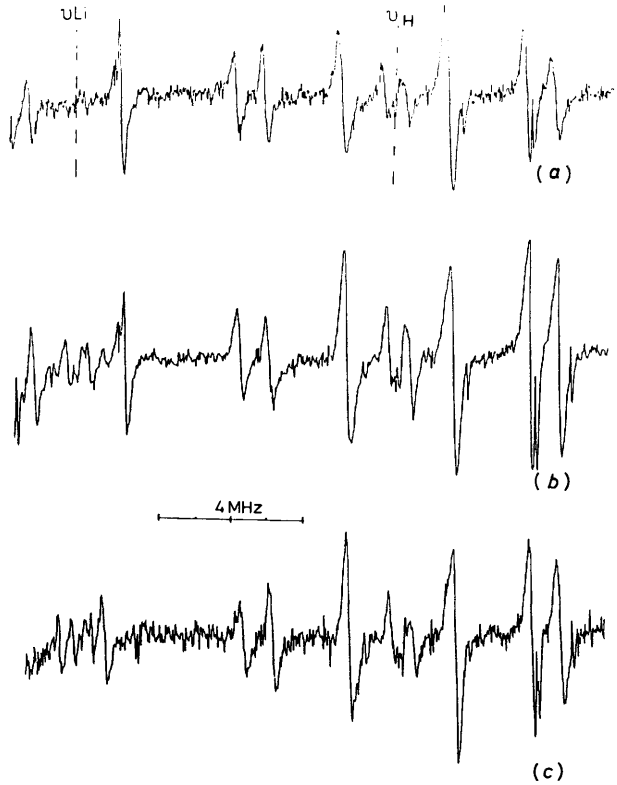

Figure 2. ENDOR spectra of $[(1)^{-\bullet}Li^+]$ in THF at 203 K obtained with different field settings.

isotopes with different magnetic moments and nuclear spins. In addition, a marked influence of the temperature on the ESR spectra of these ion pairs is observed.

In order to obtain more information about the structure of these species, ENDOR and TRIPLE resonance measurements have been performed. The experimental difficulty in detecting the ^{39}K, and ^{85}Rb ENDOR lines due to their low magnetic moments, even with powerful ENDOR spectrometers, is well known.[7] Thus, only Li, Na, ^{87}Rb, and Cs hfs constants have been determined by ENDOR, at temperatures between 178 K and 243 K. Figure 2 depicts three different ENDOR spectra of $[(1)^{-\bullet}Li^+]$ in tetrahydrofuran (THF) at 203 K obtained by irradiating different lines of the ESR spectra. Besides the line pairs symmetrically displayed about the free proton frequency, three pairs of lines, centred around the free lithium frequency, are observed, allowing the identification of three different ion pairs.

The relative intensities of these pairs of lines depend on the particular ESR line irradiated. When some frequencies in the ESR spectrum are irradiated only one pair of lines is observed as is shown in Figure 2(*a*). The relative signs of the hfs constants are determined by general TRIPLE resonance experiments according to well-known criteria.[9]

The values of the hfs determined by ENDOR and TRIPLE resonance in THF at 203 K for all the alkali ion pairs are shown in Table 1 together with those obtained by simulation of the ESR spectrum of the free radical anion in DMF, obtained by electrolytical reduction. The assignments were based on theoretical calculations, as discussed later. The value of the potassium hfs determined by ESR simulation is also included but in this case the sign is obviously undetermined. The largest effect of the cation on the proton hfs is observed for lithium ion pairs. The proton hfs for the remaining ion pairs are almost invariant.

The observation of three different alkali-metal hfs in some ketyls $[(1)^{-\bullet}M^+]$ encouraged us to extend these experiments to

Table 1. Experimental hfs constants in mT of $(1)^{-\bullet}$ obtained by electrolytical reduction in DMF at room temperature and $[(1)^{-\bullet}M^+]$ (M = Li, Na, K, Rb, Cs) in THF at 203 K determined by ENDOR and TRIPLE resonance.

	Carbon atoms						Metal ion
	1,8	3,6	2,7	4,5	9,12	10,11	a_M
$(1)^{-\bullet}$ Exp.[a]	−0.325	−0.251	0.106	0.085	−0.025	−0.010	
$(1)^{-\bullet}$ Calc.[b]	−0.308	−0.286	0.109	0.083	−0.053	−0.009	
$[(1)^{-\bullet}Li^+]$ $g = 2.0034 \pm 0.0001$	−0.329	−0.270	+0.110	+0.110	−0.024	−0.010	+0.021 −0.050 +0.094
$[(1)^{-\bullet}Na^+]$ $g = 2.0035 \pm 0.0001$	−0.333	−0.255	+0.105	+0.091	−0.026	−0.013	+0.034 +0.080 −0.12
$[(1)^{-\bullet}K^+]$ $g = 2.0035 \pm 0.0001$	−0.333	−0.253	+0.104	+0.088	−0.025	−0.013	0.021[a]
$[(1)^{-\bullet}Rb^+]$	−0.333	−0.252	+0.103	+0.088	−0.023	−0.013	(^{87}Rb) 0.1 (^{87}Rb) 0.2
$[(1)^{-\bullet}Cs^+]$ $g = 2.0034 \pm 0.0001$	−0.333	−0.251	+0.102	+0.088	−0.023	−0.009	0.013 0.038

[a] hfs constants obtained by ESR simulation, the signs were not determined. [b] McLachlan's calculations with the following parameters: $\delta_O = 2.2$; $\gamma_{CO} = 1.2$; $\gamma_{14,19} = \gamma_{16,19} = 0.85$; $\gamma_{13,17} = \gamma_{15,18} = 0.8$; $Q^H_{CH} = -2.7$ mT.

Table 2. Experimental hfs constants in mT determined by ENDOR and TRIPLE resonance of $[(2)^{-\bullet}M^+]$ (M = Li, Na, K, Rb, Cs) in THF at 193 K.

	Carbon atoms					Metal ion
	1,8	3,6	2,7	4,5	9,10	a_M
$[(2)^{-\bullet}Li^+]$ $g = 2.0033 \pm 0.0001$	−0.359	−0.323	+0.092	+0.056	+0.030	+0.021 −0.141 +0.106
$[(2)^{-\bullet}Na^+]$ $g = 2.0035 \pm 0.0001$	−0.355	−0.312	+0.080	+0.030	+0.030	+0.027 +0.061 −0.152
$[(2)^{-\bullet}K^+]$ $g = 2.0035 \pm 0.0001$	−0.353	−0.312	+0.080	+0.030	+0.030	0.015[a]
$[(2)^{-\bullet}Rb^+]$ $g = 2.0035 + 0.0001$	−0.350	−0.301	+0.078	+0.030	+0.030	(^{87}Rb)0.032 (^{87}Rb)0.251
$[(2)^{-\bullet}Cs^+]$ $g = 2.0035 \pm 0.0001$	−0.350	−0.301	+0.078	+0.030	+0.030	0.196
$(2)^{-\bullet}$ (Calculated)[b]	−0.357	−0.300	+0.121	+0.053	+0.016	

[a] Determined by ESR spectral simulation. [b] McLachlan's spin density calculation with the following parameters: $\delta_O = 2.2$; $\gamma_{CO} = 1.2$; $\gamma_{12,15} = \gamma_{14,15} = 0.85$; $\gamma_{9,11} = \gamma_{10,13} = 0.8$; $\gamma_{9,10} = 0.9$; $Q^H_{CH} = -2.7$ mT.

the other related ketones (**2**) and (**3**). In Tables 2 and 3 the values of the hfs constants determined by ENDOR and TRIPLE resonance, respectively, for $[(2)^{-\bullet}M^+]$ and $[(3)^{-\bullet}M^+]$ in THF at 193 K are shown. Also in these non-planar ketyls three different kinds of ion pairs are observed. The assignments in Tables 2 and 3 were based on theoretical spin-density calculations.

These studies have been extended to other solvents such as 2-methyltetrahydrofuran (MTHF) and 1,2-dimethoxyethane (DME) and to temperatures ranging from 173 K to room temperature. The results obtained point to a near-invariance in the proton hfs with either solvent or temperature, whereas a measurable dependence of the alkali metal hfs is observed. We have omitted the numerical values of the measured proton hfs constants at different temperatures and in different solvents for the sake of brevity. The variation of lithium and sodium hfs with temperature and solvent for $[(1)^{-\bullet}M^+]$ (M = Li, Na) is shown in Figure 3. For $[(2)^{-\bullet}M^+]$ and $[(3)^{-\bullet}M^+]$ an identical variation of the alkali metal hfs with the temperature is observed as is shown in Figure 4.

Discussion

The best fit of the experimental proton hfs shown in Tables 1 and 2 for $(1)^{-\bullet}$ and $(2)^{-\bullet}$ with those calculated by Hückel–McLachlan's method, was achieved with the parameters $\delta_O = 2.2$ and $\gamma_{CO} = 1.2$ whereas for $(3)^{-\bullet}$ the adjusted parameters are, respectively, $\delta_O = 1.9$ and $\gamma_{CO} = 1.6$ (Table 3) similar to the values referred in the literature for other ketones such as benzophenone. These values point, for the benzotropones (**1**) and (**2**), to a very high negative charge density on the oxygen atom (higher δ_O) and a larger bond length for the CO bond (lower γ_{CO}), than usual. The strong electron-donating influence

Table 3. Experimental hfs constants in mT determined by ENDOR and TRIPLE resonance of $[(3)^{-\bullet}M^{+}]$ (M = Li, Na, K, Rb, Cs) in THF at 193 K.

	Carbon atoms						Metal ion
	1,8	3,6	2,7	4,5	9,10 (ax)	9,10 (eq)	a_M
$[(3)^{-\bullet}Li^{+}]$ $g = 2.0035 \pm 0.0001$	−0.307	−0.363	+0.076	+0.096	+0.329	+0.036	+0.019 −0.137 +0.106
$[(3)^{-\bullet}Na^{+}]$ $g = 2.0036 \pm 0.0001$	−0.299	−0.359	+0.070	+0.093	+0.313	+0.030	+0.027 +0.076 −0.213
$[(3)^{-\bullet}K^{+}]$ $g = 2.0036 \pm 0.0001$	−0.292	−0.358	+0.069	+0.090	+0.305	+0.027	0.027[a]
$[(3)^{-\bullet}Rb^{+}]$ $g = 2.0036 \pm 0.0001$	−0.292	−0.358	+0.069	+0.090	+0.305	+0.027	(^{87}Rb) 0.05 (^{87}Rb) 0.11
$[(3)^{-\bullet}Cs^{+}]$ $g = 2.0034 \pm 0.0001$	−0.292	−0.358	+0.069	+0.090	+0.305	+0.027	0.222
$(3)^{-\bullet}$ (Calculated)[b]	−0.268	−0.347	+0.088	+0.098	+0.288		

[a] Determined by ESR spectral simulation. [b] McLachlan's spin density calculation with the following parameters: $\delta_O = 1.9$; $\gamma_{CO} = 1.6$; $\gamma_{12,15} = \gamma_{14,15} = 0.9$; $\delta_{11,13} = -0.1$; $Q^{H}_{CH} = -2.7$ mT; $Q^{H}_{C\text{-}CH_3} = 2.7$ mT.

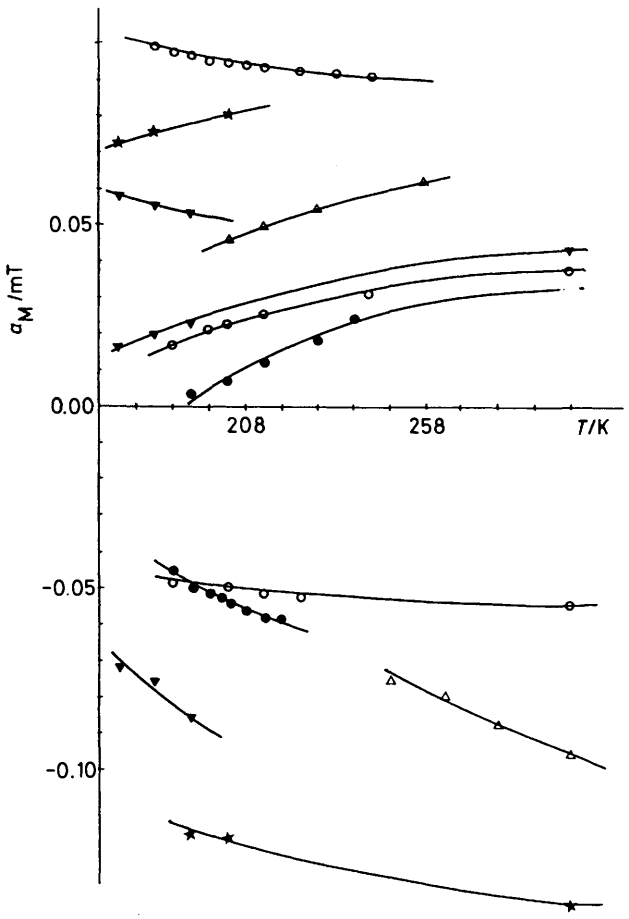

Figure 3. Experimental temperature dependence of metal hfs constants of $(1)^{-\bullet}M^{+}$ in different ethereal solvents: ▼, Li/MTHF; ○, Li/THF; ●, Li/DME; △, Na/DME; ✱, Na/THF.

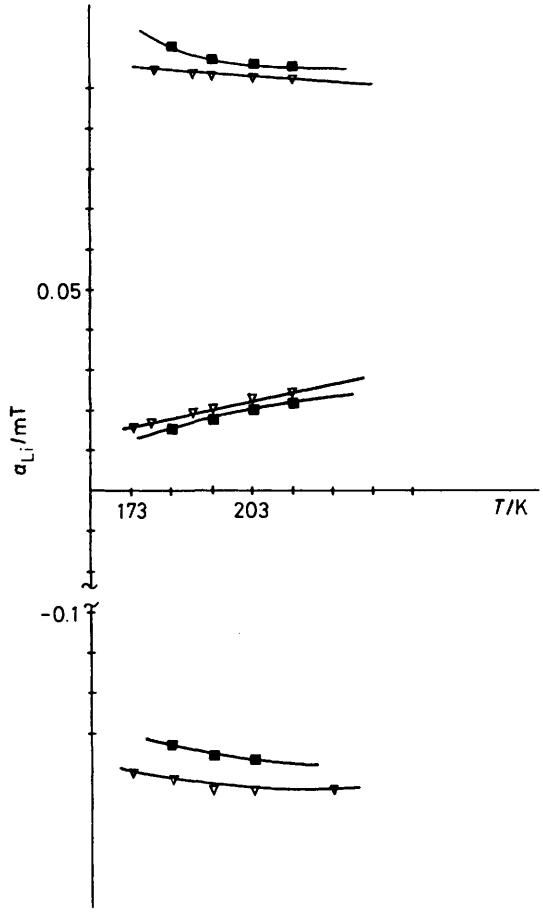

Figure 4. Experimental temperature dependence of lithium hfs constants of $[(2)^{-\bullet}Li^{+}]$ (▽) and $[(3)^{-\bullet}Li^{+}]$ (■) in THF.

of the cycloheptatrienyl ring adjacent to the carbonyl explains this different carbonyl structure.

The analysis of the proton hfs constants of the different alkali ion pairs derived from (**1**)–(**3**) shown in Tables 1–3 evidences only a weak dependence of these hfs on the counter-ion. McLachlan's spin densities calculated for $[(1)^{-\bullet}M^{+}]$–$[(3)^{-\bullet}M^{+}]$ with larger δ_O values than the one used for the free radical anion also show a weak dependence of the proton hfs constants on δ_O as is shown in Figure 5 for $[(1)^{-\bullet}M^{+}]$. These theoretical results are thus in good agreement with the experimental results given above.

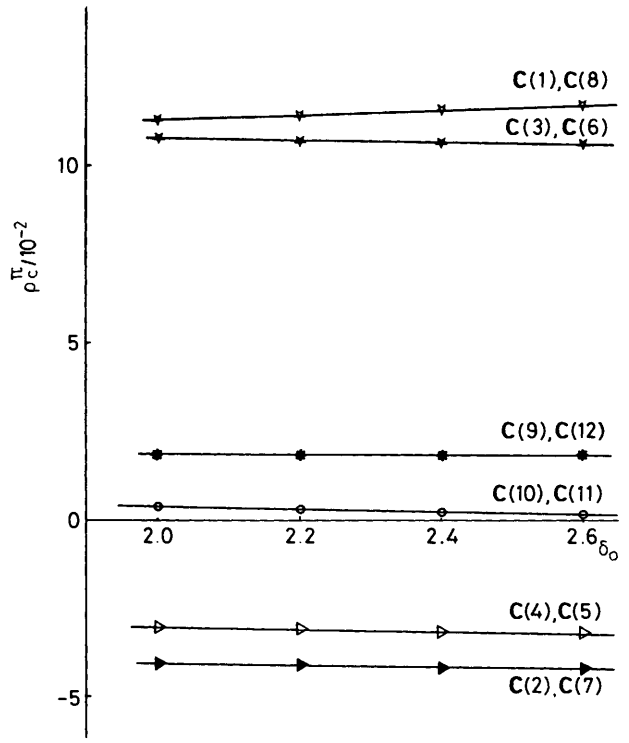

Figure 5. Spin densities calculated by McLachlan's method for $(1)^{-\bullet}$ as a function of δ_O (the other parameters used in the calculations are referred to in Table 1).

The lack of symmetry in the ESR spectra of lithium and sodium ion pairs of ketones (**1**)–(**3**) together with the presence of three different alkali-metal hfs constants measured by ENDOR/TRIPLE resonance show that the observed signals are the superposition of three different ion pairs.

For a theoretical interpretation of these results, the calculation of the spin density at the alkali-metal nucleus is necessary. INDO calculations [10] seem to be the most adequate method for large molecules though they are restricted to lithium complexes. The main problem in these calculations is obviously the uncertainty in the actual geometry of the radical anion. The X-ray structure for (**2**) has been published [11] and shows a folded conformation of the central ring as expected. In the related ketones (**1**) and (**3**), enhanced folding of the central ring is predictable [in (**1**) due to the extra phenyl ring and in (**3**) due to the presence of two sp^3 carbon atoms in the seven-membered ring]. The radical anion structure in solution is, of course, not identical with the X-ray structure for the neutral molecule. This is due not only to the existence of packing effects in the crystal, but also to the extra electron in the radical anion. A minor distortion from planarity in the radical anion in solution is consequently expected. Due to the strong affinity of the lithium cation for the carbonyl oxygen in these ketyls, as referred to above, not only is the solvation of the ion pair weaker than usual but energy barriers are conceivably of a sufficient height to inhibit the interconversion between structurally different ion pairs on the ESR time scale. For larger cations, however, the weaker interionic interaction might allow other interpretations to be considered. Following the above considerations, the most adequate way to explain the different structures of the alkali ion pairs for the ketones (**1**)–(**3**), is to consider the three different stereoisomers of Figure 6 where the solvent molecules are ignored.

Different INDO calculations based on a structure for the radical anion similar to that reported for (**2**), with small adjustments either in dihedral angles or bond lengths, have been performed. In Figure 6 the co-ordinate system as well as the geometry of the carbon skeleton in the seven-membered ring, used in the calculations are indicated for the three ion-pair

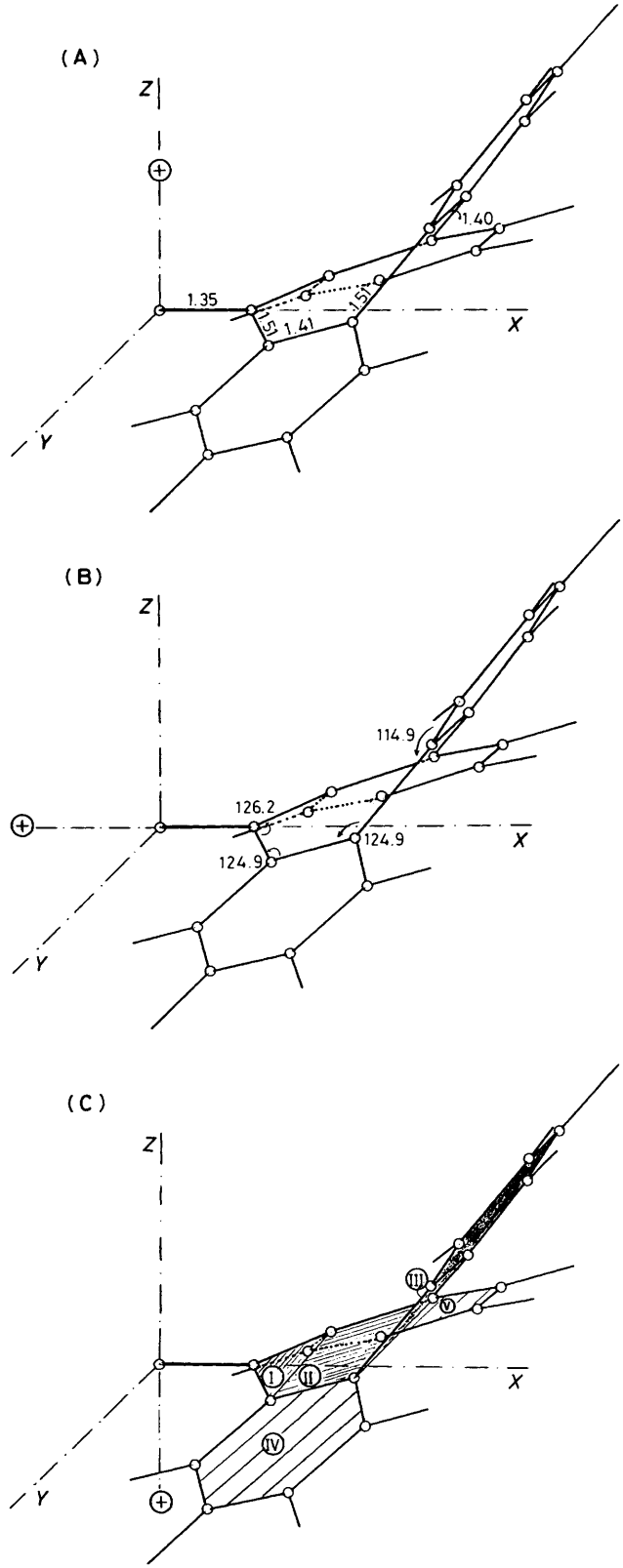

Figure 6. Ion-pair structures for the different stereoisomers of $[(1)^{-\bullet}Li^+]$. Molecular geometry assumed in the INDO calculations is indicated: bond lengths (in structure **A**), bond angles (in structure **B**), and dihedral angles (in structure **C**): i–ii, 160°; ii–iii, 155°; iv–v, 160°.

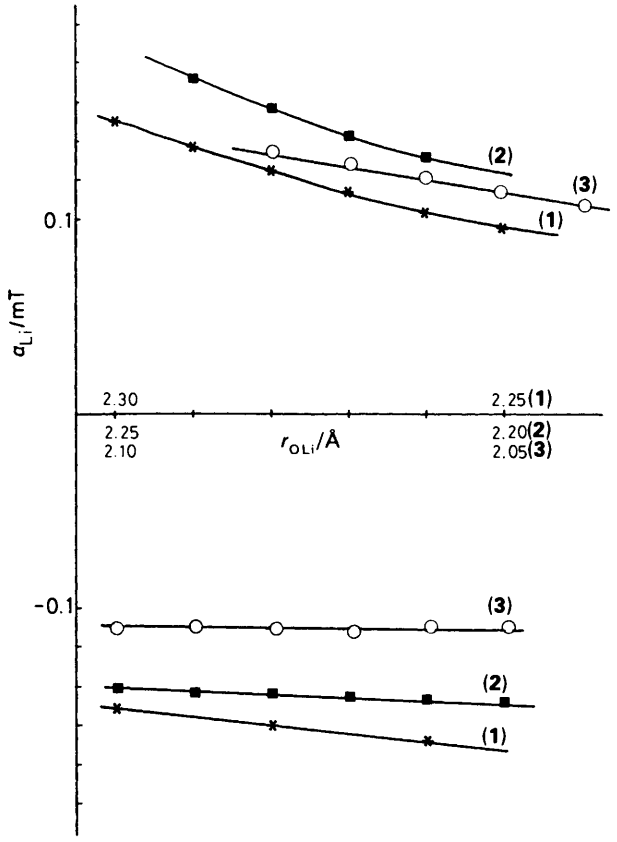

Figure 7. Calculated (INDO) lithium hfs constants in mT as a function of r_{OLi} for stereoisomers **A** and **C** of $(1)^{-\bullet}Li^{+}$–$(3)^{-\bullet}Li^{+}$.

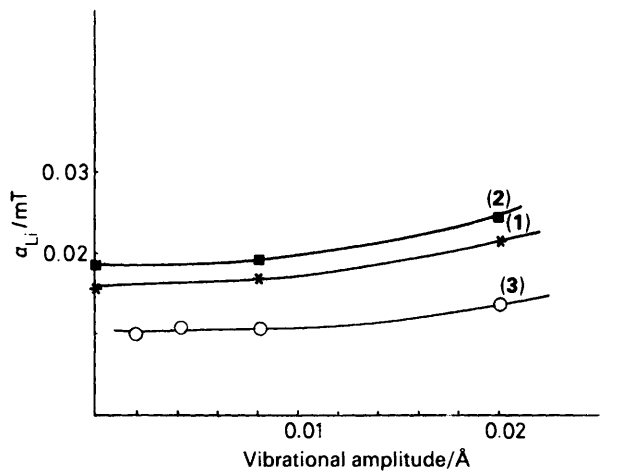

Figure 8. Calculated (INDO) lithium hfs constants in mT as a function of Li^{+} vibrational amplitude in the XZ plane, for stereoisomer **B** of $[(1)^{-\bullet}Li^{+}]$–$[(3)^{-\bullet}Li^{+}]$.

structures. For the phenyl rings the standard bond lengths and bond angles were used. The distance r_{OLi}, between the oxygen carbonyl atom and the lithium nucleus, has also been varied between 1.85 and 2.5 Å. Besides obviously the r_{OLi} distance, the structural feature with the greatest influence on the calculated lithium spin density is the carbonyl bond length. The best results were achieved with a carbonyl bond length of 1.35 Å.

A comment on this point must be made. In spite of the great similarity in all CO bond lengths measured for neutral ketones by X-ray diffraction (1.22 Å for fluorenone as well as for benzophenone and tropones) extra negative charge in the corresponding ketyls will lead not only to longer CO bonds but also to dissimilarities between them. The CO bond length in these ketyls is mainly controlled by the aromaticity demands of the adjacent groups. Whereas in the fluorenone (Fl) ketyl this lengthening is moderated by the adjacent five-membered ring which attracts the negative charge, in (**1**) and (**2**) an enhanced lengthening of the CO bond is expected due to the releasing effect of the adjacent cycloheptatrienyl ring. In (**3**), similarly to benzophenone (Bp), this effect is non-existent. Thus, the following order for CO bond lengths in ketyls is predictable:

$$CO(Fl) < CO(3) < CO[(1),(2)]$$

An even more pronounced increase in the CO bond length is expected in the corresponding dianions.

Due to the difficulties in growing crystals from ketyls, the X-ray structure for the $Fl^{-\bullet}Na^{+}$ has only recently been published.[4] The measured CO bond length 1.28 Å is longer than that measured for the neutral ketone. For (**1**)–(**3**), values higher than 1.28 Å are then expected. Another numerical value for a CO bond length reported in the literature[12] is that for $[Bp^{2-}2Li^{+}]$ where the measured value is 1.40 Å. Thus the values for carbonyl bond lengths fitted in the INDO calculations in this work, namely, 1.35 Å for $[(1)^{-\bullet}Li^{+}]$ as well as for $[(2)^{-\bullet}Li^{+}]$ and 1.31 Å for $[(3)^{-\bullet}Li^{+}]$ are in good agreement with previous considerations. The carbonyl parameters (δ_O and γ_{CO}) used in McLachlan's calculations in order to obtain the best fit with the experimental results [$\delta_O = 2.2$ and $\gamma_{CO} = 1.2$ for $(1)^{-\bullet}$ and $(2)^{-\bullet}$ and $\delta_O = 1.9$ and $\gamma_{CO} = 1.6$ for $(3)^{-\bullet}$] are also justified by the above considerations.

Table 4 shows the best values of the hfs calculated by INDO for the three different ion pair structures of Figure 6 for the ketones (**1**)–(**3**), to fit the experimental results (see Tables 1–3). As is usually the case, the INDO calculated proton hfs are in poorer agreement with the experimental ones, than those calculated by McLachlan's method. The lithium co-ordinates are indicated in the footnotes of Table 4.

The assignment of each ion pair structure to the different experimental lithium hfs constant comes from several considerations.

(*i*) In stereoisomer **A** of Figure 6, where the lithium cation lies above the oxygen atom on the concave side of the central ring, the calculated lithium hfs is negative for r_{OLi} distances ranging from 1.85 to 2.42 Å. Since, from the published X-ray structures of lithium compounds, r_{OLi} distances greater than 2.42 Å are not frequently observed, the ion-pair structure **A** may correspond to the observed negative lithium hfs.

(*ii*) In stereoisomer **B**, where the lithium cation lies along the C–O axis, the calculated lithium hfs is negative for r_{OLi} from 1.85 to 2.28 Å and positive from 2.28 Å. This stereoisomer may correspond to the ion pair with a small positive lithium hfs constant since the negative one is probably associated with stereoisomer **A**.

(*iii*) In stereoisomer **C**, with the Li^{+} above the oxygen atom on the convex side of the central ring, the calculated lithium hfs is negative for r_{OLi} ranging from 1.85 to 1.95 Å, and increasingly positive from 1.95 Å onwards. To this ion-pair structure the largest experimental positive lithium hfs may be assigned, as, for $r_{OLi} = 2.25$ Å, the calculated value is in good agreement with the experimental value. For the ketones (**2**) and (**3**) the assignment was made using similar reasoning.

As we are dealing with strongly associated ion pairs, the temperature variation may cause only small changes in the r_{OLi} distance, depending on the solvation demands. An increase in the temperature leads to a less solvated ion pair and the more loosely solvated cation can either get nearer to the radical anion (smaller r_{OLi}) or vibrate in the field of the radical anion around the equilibrium position with a larger amplitude. For

Table 4. Calculated hfs constants (mT) for [(1)$^{-\bullet}$Li$^+$]–[(3)$^{-\bullet}$Li$^+$] by INDO.

		Carbon atoms						a_{Li}	
	Configuration	1,8	3,6	2,7	4,5	9,12	10,11	Calc.	Exp.
[(1)$^{-\bullet}$Li$^+$]	A[a]	−0.258	+0.140	−0.197	+0.157	−0.015	−0.003	−0.152	−0.050
	B[b]	−0.296	+0.165	−0.229	+0.174	−0.024	−0.002	+0.016	+0.021
	C[c]	−0.252	+0.154	−0.215	+0.159	−0.021	−0.002	+0.095	+0.094
[(2)$^{-\bullet}$Li$^+$]	A[d]	−0.284	+0.158	−0.215	+0.174	+0.10 (9, 10)		−0.148	−0.141
	B[e]	−0.303	+0.171	−0.235	+0.178	+0.138		+0.019	+0.021
	C[f]	−0.264	+0.161	−0.224	+0.159	+0.132		+0.133	+0.106
[(3)$^{-\bullet}$Li$^+$]	A[g]	−0.270	+0.147	−0.215	+0.170	+0.358 (ax) +0.047 (eq)		−0.110	−0.137
	B[h]	−0.282	+0.159	−0.234	+0.172	+0.484 (ax) +0.068 (eq)		+0.017	+0.019
	C[i]	−0.247	+0.154	−0.227	+0.157	+0.461 (ax) +0.060 (eq)		+0.112	+0.106

Lithium co-ordinates in Å: [a] Li (0; 0; +2.30). [b] Li (−2.282; 0; 0). [c] Li (0; 0; −2.25). [d] Li (0; 0; +2.21). [e] Li −(2.166; 0; 0). [f] Li (0: 0; −2.21). [g] Li (0; 0; +205). [h] Li (−2.018; 0; 0). [i] Li (0; 0; −2.05).

stereoisomers **A** and **C**, the calculations made assuming the preferential vibration to be along the *Y*-axis lead to an invariant lithium hfs. The mode of vibration along the *X*-axis must be sterically hindered and has not been considered in the calculations. The temperature dependence can in these cases be explained in terms of variable r_{OLi} as is shown in Figures 7 and 8. The experimentally observed decrease of the largest positive lithium hfs, and the increase of the negative one, with increasing temperature (see Figure 3) are well interpreted theoretically by the trends shown.

The observed increase with increasing temperature of the smallest positive lithium hfs (stereoisomer **B**) is not easily interpreted in terms of a decrease in r_{OLi}. In this isomer where the cation lies along the CO bond, there is no restriction to the vibrational motion of the cation, either along the *Y*-axis or the *Z*-axis. As in the stereoisomers **A** and **C**, the spin density calculated for the lithium cation assuming the vibration along the *Y*-axis with different amplitudes is invariant. Nevertheless, the calculations made considering the vibration along the *Z*-axis indicate that with increasing amplitude of the motion there will be an increase in the lithium hfs as is shown in Figure 8. The experimentally observed increase of the smallest positive lithium hfs constant with increasing temperature may be explained in this way.

Until recently the accuracy of the position of the lithium cation relative to the fluorenone radical anion in solution proposed by Lubitz[7] was not wholly trusted. According to his calculations, the metal cation lies above the CO bond nearer to C(9) than to oxygen in the symmetry plane perpendicular to the fluorenone ring system (*i.e.* the angle C(9)–O–M <90°). In the crystalline dimer of fluorenone–sodium [Fl$^{-\bullet}$Na$^+$(DME)$_2$]$_2$ studied by Bock *et al.*[4] the same angle is 141° for the sodium cation nearest to the oxygen atom of the given radical anion. According to these authors this would also fit the ESR/ENDOR parameters in solution.

By determining experimentally the ESR/ENDOR data for three different stereoisomers in the ion pairs derived from benzotropones, and establishing for which positions the INDO calculations give the best fit for the experimental parameters in each case, we feel more confident about these results, as if we were fitting results of the calculations to the parameters of one single species. Our results are, however, so consistent with those of Lubitz[7] that we consider that they fully support his proposal. The position, however, of the sodium cations in the crystal structure of [Fl$^{-\bullet}$Na$^+$(DME)$_2$]$_2$ differs from the structure of ion pairs in solution, mainly in that the angle C(9)–O–Na is larger than 90°.

Experimental

Tribenzotropone was synthesised and purified as described in the literature.[13] * The ketones (**2**) and (**3**), supplied by Aldrich, were purified before use. 2-Methyltetrahydrofuran (MTHF), tetrahydrofuran (THF), dimethoxyethane (DME), and *N*,*N*-dimethylformamide (DMF) were dried by known techniques.

Tetrabutylammonium perchlorate (BDH) was dried *in vacuo* at 100 °C using P_2O_5 as the drying agent.

Cyclic voltammetry was performed on a Princeton Applied Research potentiostat–galvanostat model 173, with current follower 176 and universal programmer model 175, at room temperature using tetrabutylammonium perchlorate (0.1 mol dm^{-3}) as the supporting electrolyte. The working electrode was a mercury drop electrode and the reference was a saturated calomel electrode.

The samples for ESR study by electrolytical reduction were obtained by applying an increasing direct current voltage to dilute (*ca.* 5 × 10^{-4} mol dm^{-3}), oxygen- (and moisture-) free solutions in DMF, containing 0.1 mol dm^{-3} tetrabutylammonium perchlorate. Electrolyses were performed in the cavity of the spectrometer.

The solutions of the ketyls were prepared by reduction of compounds (**1**)–(**3**) with the different alkali metals (Li, Na, K, Rb, and Cs) in either MTHF, THF, or DME, by known techniques.

ESR spectra were run on a Bruker ER 200D spectrometer equipped with a variable temperature unit ER400VT. ENDOR and TRIPLE resonance experiments were run on a Bruker EN810 spectrometer.

ESR spectra were computer simulated until the match with the experimental spectra could not be further improved.

Acknowledgements

We thank the Instituto Nacional de Investigação Científica INIC, Portugal for financial support through Centro de

* One may omit the two last steps in the synthesis, which corresponds to catalytic hydrogenation of 9,12-epoxy-9,12-dihydrotribenzotropone (**4**) followed by H_2O elimination, since the reduction of (**4**) with the alkali metals leads first to the primary radical anion pair [(**4**)$^{-\bullet}$M$^+$] and then to [(**1**)$^{-\bullet}$M$^+$].

Processos Químicos da Universidade Técnica de Lisboa. The donation of a Bruker ER 200D ESR spectrometer by the Federal Republic of Germany through Gesellschaft für Technische Zusammenarbeit and of a Bruker EN810 ENDOR unit by the Foundation Volkswagenwerke is gratefully acknowledged.

References

1 A. Hoekstra, T. Spoelder, and A. Vos, *Acta Crystallogr., Sect. B*, 1972, **28**, 14.
2 J. J. Mooji, A. A. K. Klaassen, E. de Boer, H. M. L. Degens, T. E. M. Van den Hark, and J. H. Noordik, *J. Am. Chem. Soc.*, 1976, **98**, 680.
3 J. H. Noordik, J. Schreurs, R. O. Gouid, J. J. Mooji, and E. de Boer, *J. Phys. Chem.*, 1978, **82**, 1105.
4 H. Bock, H-F. Herrmann, D. Fenske, and H. Goesmann, *Angew. Chem., Int. Ed. Engl.*, 1988, **27**, 1067.
5 L. Pedersen, and R. G. Griffin, *Chem. Phys. Lett.*, 1970, **5**, 373.
6 P. Cremashi, A. Gamba, G. Morosi, C. Oliva, and M. Simonetta, *J. Chem. Soc., Faraday Trans. 2*, 1975, **71**, 1829.
7 W. Lubitz, M. Plato, K. Möbius, and R. Biehl, *J. Phys. Chem.*, 1979, **83**, 3402.
8 B. J. Tabner and J. R. Zdysiewicz, *J. Chem. Soc., Perkin Trans. 2*, 1973, 811.
9 H. Kurreck, B. Kirst, and W. Lubitz, *Angew. Chem., Int. Ed. Engl.*, 1984, **23**, 173.
10 J. A. Pople and D. L. Beveridge, 'Approximate Molecular Orbital Theory,' McGraw-Hill, New York, 1970.
11 Y. Oddon, N. Darbon, J. P. Reboul, B. Cristan, J. C. Soyfer, and G. Pèpe, *Acta Crystallogr., Sect. B*, 1984, **40**, 524.
12 B. Bogdanovic, C. Krüger, and B. Wermeckes, *Angew. Chem., Int. Ed. Engl.*, 1980, **19**, 817.
13 W. Tochtermann, K. Oppenländer, and V. Walter, *Chem. Ber.*, 1964, **87**, 1329.

Paper 9/03190A
Received 27*th July* 1989
Accepted 27*th October* 1989